White, M., Sayma, A. I. & Markides, C. (2017). Supersonic flow of non-ideal fluids in nozzles: An application of similitude theory and lessons for ORC turbine design and flexible use considering system performance. Journal of Physics: Conference Series, 821(1), 012002. doi: 10.1088/1742-6596/821/1/012002

CITY UNIVERSITY LONDON

EST 1894

City Research Online

Original citation: White, M., Sayma, A. I. & Markides, C. (2017). Supersonic flow of non-ideal fluids in nozzles: An application of similitude theory and lessons for ORC turbine design and flexible use considering system performance. Journal of Physics: Conference Series, 821(1), 012002. doi: 10.1088/1742-6596/821/1/012002

Permanent City Research Online URL: http://openaccess.city.ac.uk/17340/

Copyright & reuse

Versions of research

Enquiries

You may also be interested in:

Comparison of Different Measurement Techniques and a CFD Simulation in Complex Terrain
Christoph Schulz, Martin Hofsäß, Jan Anger et al.

Transient two-phase CFD simulation of overload operating conditions and load rejection in a prototype sized Francis turbine
Peter Mössinger and Alexander Jung

Design and testing of high temperature micro-ORC test stand using Siloxane as working fluid
Teemu Turunen-Saaresti, Antti Uusitalo and Juha Honkatukia

Uncertainty in airflow field parameters in a study of shock waves on flat plate in transonic wind tunnel
M L C C Reis, J B P Falcao Filho and M C C Araújo

The effect of dense gas dynamics on loss in ORC transonic turbines
FJ Durá Galiana, APS Wheeler, J Ong et al.

The Geometry of Non-Ideal Fluids
S G Rajeev

Optimization of the blade trailing edge geometric parameters for a small scale ORC turbine
L Zhang, W L Zhuge, J Peng et al.

Improving of the photovoltaic / thermal system performance using water cooling technique
Hashim A Hussien, Ali H Numan and Abdulmunem R Abdulmunem

Supersonic flow of non-ideal fluids in nozzles: An application of similitude theory and lessons for ORC turbine design and flexible use considering system performance

M White[1], A I Sayma[2] and C N Markides[1]

[1] Clean Energy Processes (CEP) Laboratory, Department of Chemical Engineering, Imperial College London, South Kensington Campus, London, SW7 2AZ, UK
[2] Department of Mechanical Engineering and Aeronautics, City University London, Northampton Square, London, EC1V 0HB, UK

Email: martin.white@imperial.ac.uk

Abstract. A significant improvement in the economy-of-scale of small-scale organic Rankine cycle (ORC) systems can arise from the appropriate design of components that can be manufactured in large volumes and implemented flexibly into a wide range of systems and potential applications. This, in turn, requires accurate predictions of component performance that can capture variations in the cycle conditions, parameters or changes to the working fluid. In this paper previous work investigating a modified similitude theory used to predict the performance of subsonic ORC turbines is extended to analyse the supersonic flow of organic fluids within 2D converging-diverging nozzles. Two nozzles are developed using a minimum length method of characteristics design model coupled to REFPROP. These are designed for R245fa and Toluene as working fluids with nozzle exit Mach numbers of 1.4 and 1.7 respectively. First, the nozzle performance is confirmed using CFD simulations, and then further CFD simulations are performed to evaluate the performance of the same nozzles over a range of different inlet conditions and with different working fluids. The CFD simulations are compared to predictions made using the original and modified similitude theories, and also to predictions made by conserving the Prandtl-Meyer function for the different operating conditions. The results indicate that whilst the modified similitude model does not accurately predict nozzle performance, conserving the Prandtl-Meyer function allows to predict the nozzle outlet Mach number to within 2% providing there is not a significant change in the polytropic index. Finally, the effect of working fluid replacement on the ORC system is discussed, and preliminary results demonstrate the possibility of matching a particular turbine to a heat source through optimal working fluid selection.

1. Introduction

The organic Rankine cycle (ORC) is a promising technology for the conversion of low temperature heat sources into mechanical work across a range of power outputs ranging from a few kW to the MW scale. However, despite successful commercialization for large-scale systems [1], implementation of smaller systems has not followed the same progress, primarily due to their high capital costs. Among other improvements such as in performance and reliability, improvements in their economy-of-scale can act as an important enabling factor in their widespread implementation. One approach to achieving this is to develop ORC systems that operate efficiently over a range of operating conditions, whilst using different working fluids. Although robust techniques do exist for the design of components that best match targeted operating conditions, the development of ORC components that can operate flexibly over a range of conditions requires methods to predict the performance of these components at design and off-design conditions.

Nomenclature

a	Speed of sound, m/s		β	Relative flow angle, °
b	Blade height, mm		θ	Flow turning angle, °
c	Fluid velocity, m/s		ρ	Density, kg/m^3
D_h	Hydraulic diameter, mm		μ	Viscosity, Pa s
h	Enthalpy, J/kg		ν	Prandtl-Meyer function, °
L	Nozzle length, mm		ν_{ts}	Isentropic velocity ratio
k	Polytropic index		η_n	Stator isentropic efficiency
$\dot{m}$	Mass flow rate, kg/s		Δh_s	Isentropic enthalpy drop, J/kg
Ma	Mach number			
N	Rotational speed, rpm		**Subscripts**	
o_{th}	Throat width, mm		*	Choked conditions
P	Pressure, kPa		0	Original operating point
R	Nozzle construction radius, mm		01	Total inlet conditions
Re	Reynolds number		2	Rotor inlet/nozzle outlet
T	Temperature, K		3	Rotor outlet
u	Rotor blade velocity, m/s		c	Condensation
Z_n	Stator blade number		d	Design
α	Absolute flow angle, °		s	Isentropic conditions

Within an ORC system, the turbine is arguably a critical component since it is responsible for generating the power within the system. ORC turbine design is complicated since the behaviour of organic fluids can significantly deviate from that of an ideal gas, thus requiring complex equations of state. Furthermore, at operation close to their critical point, organic fluids could exhibit non-classical fluid dynamic behaviour leading to expansion shocks and compression fans [2,3]. In addition, low values for the speed of sound can also result in supersonic flows at the rotor inlet and possibly at the rotor outlet. For rotor inlet Mach numbers only slightly exceeding unity, a conventional converging stator blade can be implemented with the required supersonic conditions being achieved in the rotor-stator interspace [4]. However, at higher Mach numbers, supersonic stators are required. These are constructed with a subsonic converging section that accelerates the flow to the choked conditions followed by a diverging section that expands the flow isentropically to the desired Mach number. A number of papers have addressed the design of these stators, for example Wheeler and Ong [5] who developed a stator design model using the Method of Characteristics, and Pasquale et al. [6] who constructed a stator using Bezier splines and optimized the geometry using a genetic algorithm.

Alongside the development of design methods, studies have focused on supersonic flows in ORC stators using computational fluid dynamics (CFD) [7-10]. These simulations couple either research flow solvers, or commercial CFD codes, with suitable equations of state. In the absence of experimental data for validation, these solvers were evaluated qualitatively against design models, or experimental data for ideal gas turbines. Recently, Galiana et al. [3] presented experimental results investigating trailing edge losses in ORC turbines in a Ludwieg tube. This, along with further developments in other organic vapour test facilities [11,12], is critical for the validation of CFD tools used to simulate supersonic flows in ORC turbine components.

Clearly, the added complexities of using non-ideal working fluids mean that it is not suitable to apply conventional ideal gas turbine performance prediction models, such as similitude theory, directly to ORC turbines. This has been attempted, for example in Ref. [13], but the errors introduced by using simplified methods based on the ideal gas law has been demonstrated recently [14]. The similitude concept has been applied to ORC turbines [15], but this is generally for turbine design, rather than off-design performance predictions. Previously, the present authors investigated the application of similitude theory for the prediction of subsonic ORC turbine performance and developed a modified similitude model for this purpose [16]. Equation 1 is a simplified form of this model assuming a given turbine design with a fixed geometry, where Δh_s is the isentropic enthalpy drop across the turbine, η is the turbine isentropic efficiency, $\dot{m}$ is the mass flow rate, N is the rotational speed, and a^*, ρ^* and μ are the speed of sound, density and dynamic viscosity at the

stator throat. Recently, this model has been used to show how the economy-of-scale of a small subsonic ORC turbine can be improved through appropriate operation and working fluid selection [17].

$$\left[\frac{\Delta h_s}{a^{*2}}, \eta\right] = f\left(\frac{\dot{m}}{\rho^* a^*}, \frac{\rho^* a^*}{\mu}, \frac{N}{a^*}\right) \tag{1}$$

The aim of this paper is to extend the similitude concept by considering working fluid replacement in supersonic ORC turbines, through the design and analysis of two converging-diverging nozzles for R245fa and Toluene using a minimum length nozzle design model. Nozzle performance is investigated using CFD simulations. Subsequently, methods to predict nozzle performance following a change in the working fluid are hypothesized; these involve using the modified similitude theory to predict the nozzle mass flow rate and isentropic enthalpy drop, and predicting the nozzle performance by conserving the Prandtl-Meyer function. These predictions are compared to further CFD simulations. Finally, the implications of fluid replacement on ORC system performance are discussed with the ultimate goal of improving the current economy-of-scale.

2. Method of characteristics and inviscid 2D nozzle design

To design a supersonic nozzle an inviscid 2D minimum length nozzle design model, based on the method of characteristics (MoC), is coupled to real gas equations of state to account for non-ideal fluid properties [18]. Aldo and Argrow [19] were the first to investigate minimum length nozzles for organic fluids, and the model developed here is similar. Although more sophisticated nozzle design methods have been developed more recently, for example [6], the focus of this paper is to investigate the effects of working fluid replacement on nozzle performance, rather than generating optimized geometries. Therefore, the simpler, minimum length method was deemed to be suitable. For a differential fluid element undergoing a supersonic expansion, the amount of flow turning, $d\theta$, is given by Equation 2, where c is the fluid velocity. For a perfect gas with a constant ratio of specific heats, Equation 2 can be integrated analytically to determine the Prandtl-Meyer function. However, for a non-ideal gas Equation 2 can be integrated numerically.

$$d\theta = (\sqrt{\text{Ma}^2 - 1}/c)\, dc \tag{2}$$

Before considering an ORC radial inflow turbine stator, this paper studies the flow within 2D converging-diverging nozzles. This is done not only to validate the design model, but also as a preliminary investigation into scaling effects in supersonic flows of organic fluids. Using the total inlet conditions and Mach numbers defined in Table 1 for R245fa and Toluene, the MoC model was used to design the diverging sections of two converging-diverging nozzles. These working fluids were selected since they are suitable working fluids for low temperature and high temperature ORC applications respectively [1]. The total inlet conditions were defined as 95% and 101% of the critical pressure and temperature respectively to ensure operation near the critical point where non-ideal gas effects are expected. The turbine outlet pressure was defined based on an assumed ORC condensation temperature T_c. Defining the rotor inlet absolute flow angle (α_2 = 74.5°), rotor inlet relative flow angle (β_2 = -21.8°), and isentropic velocity ratio ($\nu_{ts} = u_2/\sqrt{2\Delta h_s} = 0.68$; where u_2 is the rotor inlet blade velocity and Δh_s is the turbine isentropic total to static enthalpy drop) enables the rotor inlet velocity triangle to be determined. Finally, assuming a stator isentropic efficiency (η_n = 0.9) defines the rotor inlet conditions. The mass flow rates correspond to a radial inflow turbine with a rotor diameter of 80 mm.

Table 1. Thermodynamic cycles and turbine designs used in this study.

	T_{01} [K]	P_{01} [kPa]	$\dot{m}$ [kg/s]	Ma_2	P_2 [kPa]	b_2 [mm]	T_c [K]
R245fa	431	3469	1.76	1.4	1138	2.38	323
Toluene	598	3920	0.45	1.7	667	1.20	383

The accuracy of the MoC model depends on the number of lines used to construct the expansion fan, and the number of elements used in the numerical integration of Equation 2. A sensitivity study using n = 50, 100 and 250 was conducted for both of these parameters and it was found that 100 elements were sufficient, with maximum errors for the wall coordinates of 0.05% and 0.25% for R245fa and Toluene respectively, relative to n = 250. Figure 1 shows the final nozzle designs. The parameters used to construct the rest of the nozzle are

shown in Figure 2 and Table 2. The throat width, o_{th}, is calculated by Equation 3 with b_2 the rotor inlet blade height (Table 1), Z_{n} the number of turbine stator vanes ($Z_{\text{n}} = 16$), and ρ^* and a^* the static choked throat conditions. Equation 4 gives the design Reynolds number where D_{h} is the throat hydraulic diameter.

$$o_{\text{th}} = \dot{m}/(\rho^* a^* b_2 Z_{\text{n}}) \tag{3}$$

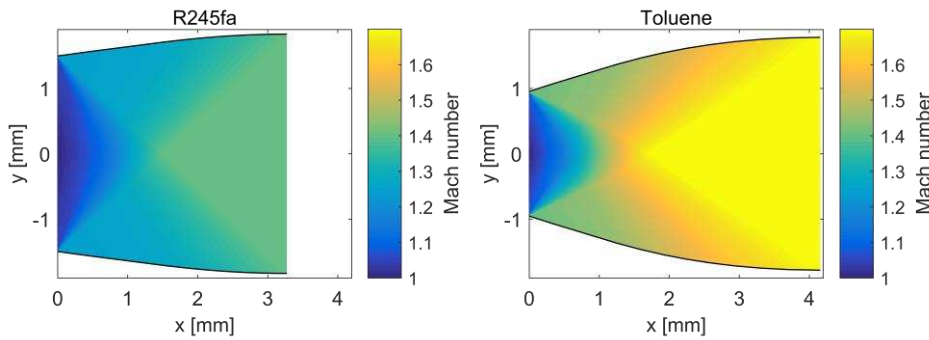$$\text{Re}_{\text{d}} = (\rho^* a^* D_{\text{h}})/\mu \tag{4}$$

Figure 1. Minimum length supersonic nozzles for the expansion of R245fa to Ma = 1.4 and Toluene to Ma = 1.7, obtained using the MoC model.
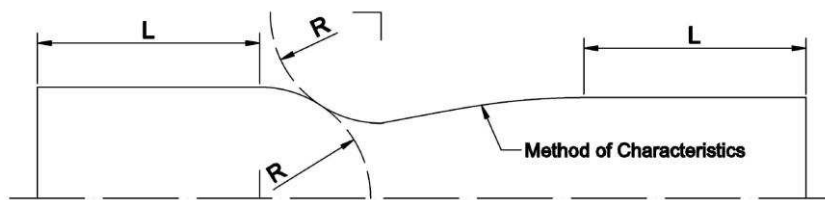

Figure 2. Geometry of the converging-diverging nozzles.

Table 2. Design parameters for the converging-diverging nozzles.

	o_{th} [mm]	R [mm]	L [mm]	Re_{d}
R245fa	2.97	2.23	8.91	$2.52{\times}10^6$
Toluene	1.89	1.41	5.66	$1.09{\times}10^6$

3. CFD simulation setup and MoC validation

A steady-state quasi-2D CFD simulation was setup in ANSYS CFX to validate the two nozzle designs. The inlet conditions were set to the total inlet conditions, the outlet was set to a supersonic outlet and the $k\text{-}\omega$ SST turbulence model with automatic wall function was selected. The meshes were constructed from $160{\times}10^3$ elements. For each nozzle design two additional meshes, consisting of $40{\times}10^3$ and $360{\times}10^3$ elements, were also constructed. It was found that the percentage error in the nozzle efficiency predicted by the original mesh compared to the finest mesh was less than 0.1% for both nozzles, thus confirming the suitability of the original meshes. Working fluid properties were accounted for by generating fluid property tables using REFPROP prior to the simulation, and a sensitivity study considering the resolution of these fluid property tables was conducted with table sizes of 50, 100 and 250. The results show that the percentage errors in the nozzle efficiency predicted for a table size of 100 compared to a table size of 250 were 0.07% and 0.04% for the R245fa and Toluene nozzles respectively. The CFD results for the R245fa and Toluene nozzles, both with a mesh size of $160{\times}10^3$ elements and fluid property table size of 100, are shown in Figure 3.

Overall, the MoC model has generated supersonic nozzles that expand the two fluids to the desired Mach numbers. Weak oblique shocks are found downstream of the diverging supersonic sections and this leads to small bumps in the midline Mach number distribution. This effect is attributed to the nozzle wall boundary layers, which effectively reduce the nozzle flow area. Boundary layer effects are not considered within the MoC model, therefore explaining the small discrepancies observed. The model can be improved by extending the nozzle wall by the boundary layer displacement thickness. However, given that the outlet Mach numbers agree to within 1%, this modification was deemed unnecessary.
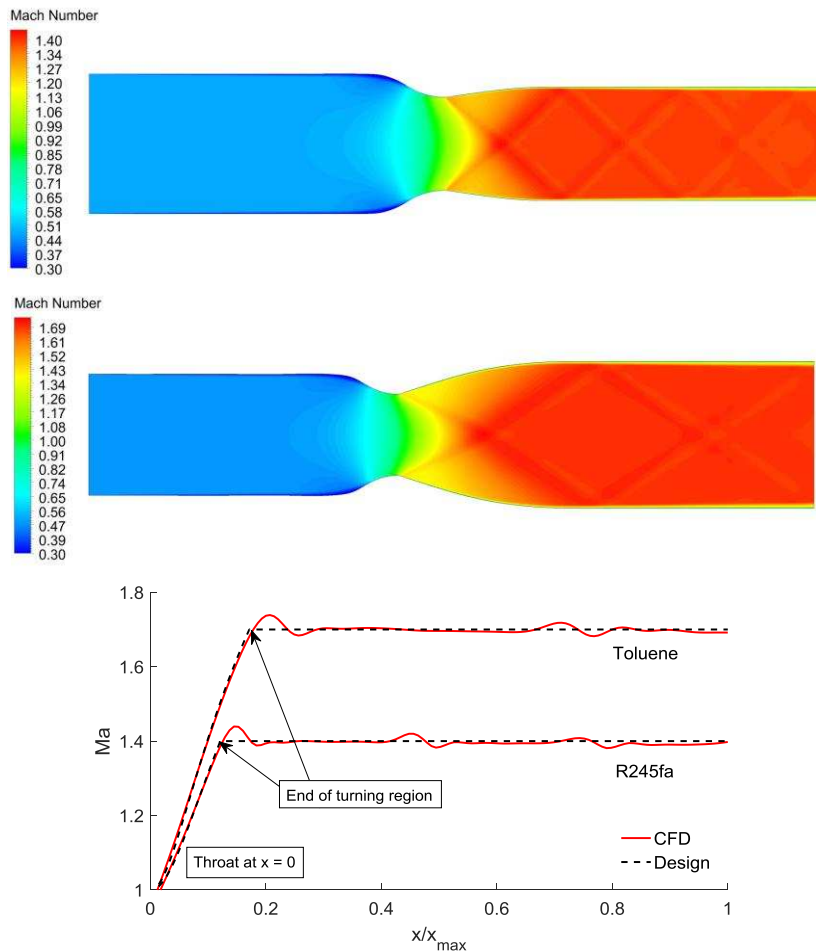
Figure 3. Validation of the MoC nozzle design model: R245fa nozzle CFD simulation (top); Toluene nozzle CFD simulation (middle); comparison between the midline Mach number distributions obtained using the MoC model and CFD simulation. Note that MoC results are only valid for $x > 0$.

4. Scaling of the supersonic nozzle

Having setup CFD simulations for both nozzles, the analysis can be extended to investigate alternative operating conditions. The first investigation considers a change in the total inlet conditions. Moving down the isentropes that correspond to the total inlet conditions defined in Table 1, alternative inlet conditions were defined at 75%, 50% and 25% of Re_d (Cases 1 to 3 in Table 3). Cases 4 to 9 correspond to changing the working fluid. For these cases it was desirable to keep Re constant, such that the effect of changing the working fluid and Re effects can be isolated from one another. Therefore, for each working fluid an isentrope was constructed that coincides with an operating point at 95% and 101% of the fluid critical pressure and temperature respectively. The throat Reynolds number was then calculated for various points along this isentrope and the nozzle inlet conditions were selected to ensure that Re remained constant. From Table 3 it can be seen that in some cases it was not possible to maintain Re. In these cases, the inlet conditions were set to the conditions that resulted in the Reynolds number that was closest to the original design point.

Using these alternative inlet conditions, a number of CFD simulations can be performed to establish nozzle performance. However, the purpose of this work is to also develop simple methods to predict nozzle performance following these changes. The first method applies the modified similitude model (Equation 1), and hypothesizes that for the same reduced head and flow coefficients, the nozzle performance will remain the same. Here the reduced head coefficient is defined as the isentropic total-to-static enthalpy drop across the nozzle normalized by the speed of sound squared $(h_{01} - h_{2s})/a^2$. In the conventional similitude model the total inlet speed of sound, a_{01}, is used whilst in the modified similitude model the choked throat speed of sound, a^* is used. Using a^* is expected to be more accurate, since the choked mass flow rate will be conserved. However, the use of a_{01} is included here as further validation of the modified similitude model. Similarly, the mass flow rate is related to the flow coefficient, $\dot{m}/\rho a$.

A second method considers the Prandtl-Meyer function, ν. Since ν is central to the supersonic nozzle design process, it is hypothesized that nozzle performance can be determined by maintaining the same amount of flow turning within the nozzle following a change in the operating conditions. For each case, the value of ν for a range of Mach numbers is shown in Figure 4.

Table 3. Alternative inlet conditions for the R245fa and Toluene nozzles.

| Case	Working fluid	R245fa nozzle			Toluene nozzle		
		T_{01} [K]	P_{01} [kPa]	Re/Re_d	T_{01} [K]	P_{01} [kPa]	Re/Re_d
1	R245fa/Toluene	411	2366	0.75	574	2684	0.75
2	R245fa/Toluene	390	1470	0.50	553	1666	0.50
3	R245fa/Toluene	364	677	0.25	526	763	0.25
4	R245fa	**431**	**3469**	**1.00**	412	2438	1.00
5	Toluene	598	3920	0.77	**598**	**3920**	**1.00**
6	MDM	570	1344	0.57	570	1344	0.74
7	R1234yf	368	3046	1.00	349	2109	1.00
8	Isopentane	465	3209	0.85	457	2811	1.00
9	R123	461	3479	0.99	439	2470	1.00
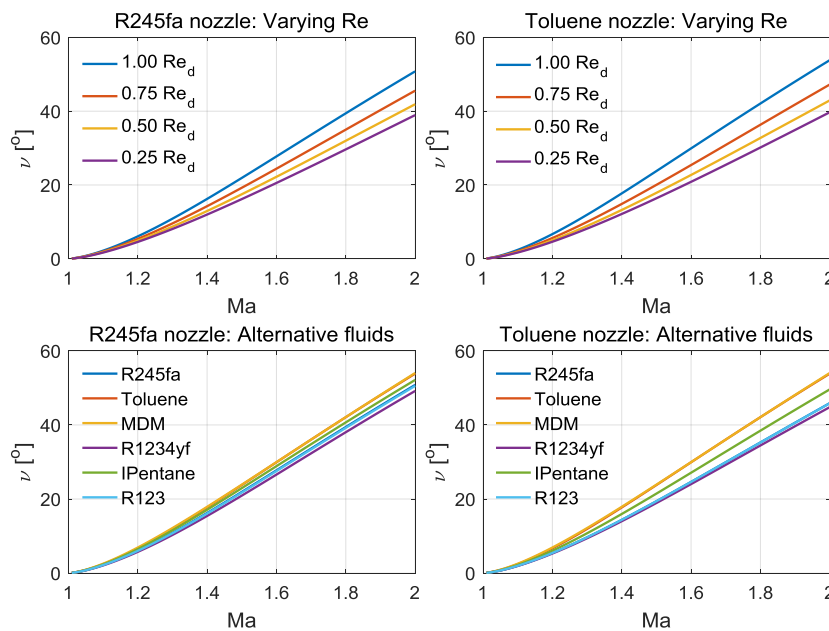
Figure 4. Prandtl-Meyer functions for: R245fa nozzle alternative inlet conditions (top-left); Toluene nozzle alternative inlet conditions (top-right); R245fa nozzle alternative fluids (bottom-left); Toluene nozzle alternative fluids (bottom-right).

For both nozzles, operating with the design fluid but at lower Reynolds numbers results in a reduction in ν for expansion to the same Mach number. Similarly, a change in the working fluid also causes a change in ν for expansion to the same Mach number. It is found that the lines for Toluene and MDM coincide, indicating that both fluids exhibit similar flow turning under similar expansion conditions. The same is found for the R245fa and R123 lines. Ultimately, Figure 4 could be used to predict the Mach number distribution within the nozzle for alternative conditions. By example, consider the centreline Mach number distribution obtained for the R245fa nozzle (Figure 3). For each x-coordinate the corresponding Mach number can be converted into a value for ν. Then for an alternative inlet condition each value of ν can be converted into the equivalent Mach number that would be required to maintain that same amount of flow turning within the nozzle.

At this point, it is suitable to discuss the work of Wheeler and Ong [5] who proposed an alternative method of obtaining ν to avoid the numerical integration of Equation 2. They assumed that during an isentropic expansion across a known pressure ratio the working fluid obeys the polytropic law $P/\rho^k =$ constant, where k is the polytropic index and can be obtained numerically using a linear regression. It was shown that as k reduces,

ν increases, resulting in a greater flow turning for expansion to the same Mach number. Using the ν conservation method described in the previous paragraph the static outlet pressures for the cases described in Table 3 can be predicted, and the values for the polytropic index can be obtained (Table 4). These values confirm the results shown in Figure 4, with cases with a higher k value corresponding to lower ν values. Furthermore, the close proximity of the MDM and Toluene lines, and the R245fa and R123 lines, are confirmed by their similar k values. Finally, it should be noted that cases 1 to 3 also correspond to significant changes in k. Therefore, when the CFD results for these cases are evaluated it will be important to identify whether any deviations are attributed to the change in Reynolds number, or the change in k.

To conclude this section, a final remark is made regarding Wheeler and Ong's work [5]. Through calculating ν based on k it was demonstrated how the shape of a supersonic nozzle changes with changes in k. Considering this, it is expected that a significant change in k will require a significantly different nozzle design. In the context of developing small-scale ORC turbines to be used within multiple applications the important question then becomes how much of a deviation in k can be tolerated before the performance of the nozzle deviates significantly from the design point.

Table 4. Polytropic index values for the similitude cases corresponding to conservation of ν.

Case	R245fa	Toluene	Case	R245fa	Toluene	Case	R245fa	Toluene
1	0.876	0.901	4	0.790	0.923	7	0.823	0.944
2	0.947	0.962	5	0.733	0.813	8	0.757	0.869
3	1.010	1.011	6	0.714	0.802	9	0.797	0.925

5. CFD results for alternative inlet conditions

CFD simulations were also performed for the cases defined in Table 3, resulting in 9 simulations per nozzle. For each simulation the centreline Mach number distribution was determined, along with the mass flow rate, mass averaged values for T_{01} and P_{01}, and the area averaged values for P_2 and Ma_2. This facilitated the calculation of the nozzle efficiency η_n (Equation 5), which ranged between 0.983 and 0.987, and 0.984 and 0.988 for the R245fa and Toluene nozzles respectively. For both nozzles the lowest efficiency was found for the $0.25Re_d$ cases, whilst the highest efficiencies were found for the highest Re_d. This was expected since lower Reynolds numbers imply thicker nozzle wall boundary layers, and a greater viscous loss.

$$\eta_n = (h_{01} - h_2)/(h_{01} - h_{2s}) \tag{5}$$

Using the CFD results, the reduced head and flow coefficients were calculated using both total ($\dot{m}/\rho_{01}a_{01}$) and choked ($\dot{m}/\rho^*a^*$) conditions. The flow coefficient based on total inlet conditions ranged between $68.9{\times}10^{-6}$ and $79.7{\times}10^{-6}$ for the R245fa nozzle, and $2.27{\times}10^{-6}$ and $2.62{\times}10^{-6}$ for the Toluene nozzle. By comparison the flow coefficient based on the choked conditions was found to be $112{\times}10^{-6}$ for all cases for the R245fa nozzle, and $3.68{\times}10^{-6}$ for all cases for the Toluene nozzle. This shows that the similitude model based on total conditions cannot predict the choked mass flow rate following a change in the working fluid or inlet conditions. By comparison, the choked conditions can accurately predict the mass flow rate. However, the head coefficients based on the choked conditions ranged between 1.08 and 1.32 for the R245fa nozzle, and 1.73 and 2.34 for the Toluene nozzle. Therefore, since the head coefficient is not the same, these results indicate that the modified similitude model cannot fully predict the supersonic nozzle performance following a change in the inlet conditions. It is therefore necessary to investigate scaling using ν.

Considering the R245fa nozzle operating at the design point (Case 4), the midline Mach number distribution obtained from CFD for that particular case can be scaled to the other 8 cases defined in Table 3 by conserving ν. This provides the predicted midline Mach number distribution for that nozzle operating under each alternative condition. These predictions can then be compared to the midline Mach number distributions obtained directly from CFD for that particular nozzle and alternative inlet condition, thereby confirming whether the conservation of ν can be used to predict nozzle performance. To conduct a thorough assessment on the suitability of the scaling method, the process was repeated using each CFD simulation as the initial starting point which is scaled to the other 8 cases. Overall, this resulted in 144 comparisons ($9{\times}8$ per nozzle) between the predictions made by conserving ν and the CFD results obtained directly from CFD. Quantitative

comparisons were done using three parameters. The first parameter k/k_0 is the change in the polytropic index where k is the polytropic index corresponding to the alternative inlet condition, and k_0 is the polytropic index associated with the original simulation used during the ν conservation. Similarly, the second parameter Re/Re_0 is the change in Reynolds numbers where Re is the Reynolds number associated with the alternative inlet conditions, and Re_0 is the Reynolds number associated with the original simulation. The final parameter was defined as the maximum percentage error between the prediction and the CFD result.

Of the 144 comparisons, Figure 5 displays 4 of these comparisons in more detail. The solid lines correspond to the predictions made by conserving ν and the dashed lines correspond to the CFD results. These comparisons have been selected to isolate the effects of varying k, and varying Re, from each other. The left plot displays comparisons made for the R245fa nozzle when $Re/Re_0 = 1$, whilst the right plot displays comparisons made for the R245fa nozzle when $k/k_0 = 1$.
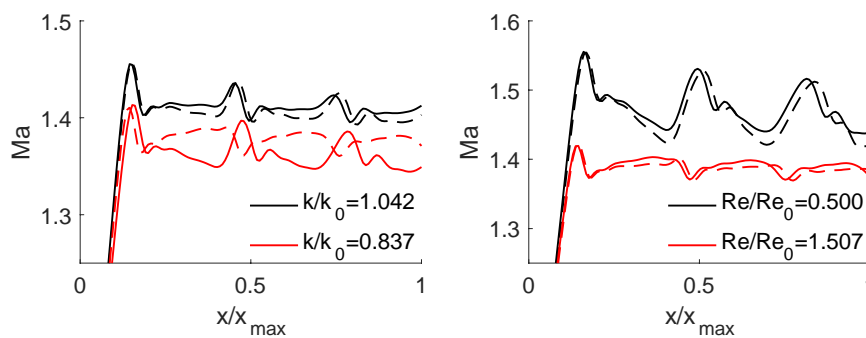

Figure 5. Comparison between centreline Mach number predicted by conserving ν (full) and CFD (dashed): R245fa nozzle, $Re/Re_0 = 1$ (left); R245fa nozzle, $k/k_0 = 1$ (right).

Firstly, it is noted that in some cases more uneven Mach number distributions are found compared to the flatter Mach number distributions shown in Figure 3. This is because a significant change in the inlet conditions can result in either under or over expansion within the nozzle, resulting in more pronounced variations in the Mach number in the straight section downstream of the diverging nozzle. Furthermore, since each case was used as a reference case to be scaled to the other 8 cases, there are situations where an off-design simulation is used during the conservation of ν (i.e. the $Re/Re_0 = 0.5$ case). Secondly, it is observed from the right plot that the ν conservation method accurately predicts the midline Mach number distribution following a change in Re, provided that k does not change. However, the left plot shows the predictions made by conserving ν are much more sensitive to a change in the polytropic index. Whilst the results for the R245fa nozzle with $k/k_0 = 1.042$ show good agreement, the $k/k_0 = 0.837$ case shows a much greater deviation. The CFD results indicate that for $k/k_0 < 1$ the flow accelerates quicker within the diverging section of the nozzle than predicted by the ν conservation method. Although not demonstrated in Figure 5, it was also observed that for $k/k_0 > 1$ the CFD results indicate the opposite, with the flow taking longer to reach the maximum Mach number. Interestingly though, both results predict the same maximum Mach number within the nozzle.

The results from all 144 comparisons are summarized in Figure 6, which is a contour plot showing the maximum percentage error in the Mach number predicted by conserving ν compared to the CFD simulation results. This plot indicates that the ν conservation method accurately predicts the midline Mach number distribution when $k/k_0 = 1$ and $Re/Re_0 = 1$. Furthermore, within the ranges of $0.9 < k/k_0 < 1.1$ and $0.5 < Re/Re_0 < 2.0$ the ν conservation method can predict the midline Mach number distribution to within 2%. Therefore, this investigation into the scaling effects in supersonic nozzles suggests that providing the change in k and Re following a change in the inlet conditions or working fluid is within this limit, the ν conservation method can accurately predict nozzle performance.

6. Implications of working fluid replacement on ORC system performance
Finally, it is important to discuss the implications of working fluid replacement on the performance of the whole ORC system. Considering the CFD results shown for the $k/k_0 = 1.042$ and $Re/Re_0 = 1.507$ cases in Figure 5, these results show a relatively flat Mach number distribution. This suggests that the flow is not significantly under or over turned at the end of curved supersonic section such that significant variations in the Mach number downstream of this point are not observed, therefore suggesting the nozzle is operating close to optimal

conditions. These $k/k_0 = 1.042$ and $\mathrm{Re}/\mathrm{Re}_0 = 1.507$ cases correspond to the R245fa nozzle operating with R1234yf and Isopentane respectively. A similar result is also obtained when this nozzle operates with R123. Therefore, based on the known nozzle outlet static pressures and absolute flow velocities, and assuming that the nozzle design can be incorporated into a suitable stator design that will deliver the flow at the desired flow angle (i.e. $\alpha_2 = 74.5°$), the turbine blade velocity for each case can be selected to ensure the same relative flow angle at the rotor inlet (i.e. $\beta_2 = -21.8°$) using Equation 6. Based on this, and assuming that the rotor operates at the same isentropic velocity ratio (i.e. $\nu_{ts} = 0.68$), the enthalpy at the turbine outlet following an isentropic expansion h_{3s} (Equation 7), and therefore, the turbine pressure ratio and ORC condensation temperature can be obtained. Finally, conserving the flow coefficient ($\dot{m}/\rho^* a^*$) supplies the mass flow rate, and in turn the expected turbine power.

$$u_2 = \mathrm{Ma}_2 a^* (\sin \alpha_2 - \cos \alpha_2 \tan \beta_2) \tag{6}$$

$$h_{3s} = h_{01} - (1/2)(u_2/\nu_{ts})^2 \tag{7}$$

This results from this analysis are plotted against the turbine inlet temperature in Figure 7. Ultimately, the results demonstrate how the same turbine could be used in applications with different heat sources by matching the working fluid to the heat source, thus providing an indication of the possibility of working fluid replacement in supersonic ORC turbines. This is a promising result that extends previous work completed for subsonic ORC turbines [17]. It should of course be noted that a slight penalty in terms of an increasing condensation temperature is observed, and future efforts should investigate this more thoroughly.
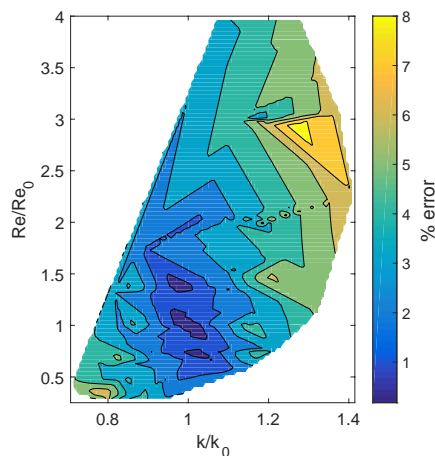

Figure 6. Maximum error in Ma predicted by conserving ν , compared to the CFD results, as a function of k/k_0 and $\mathrm{Re}/\mathrm{Re}_0$.
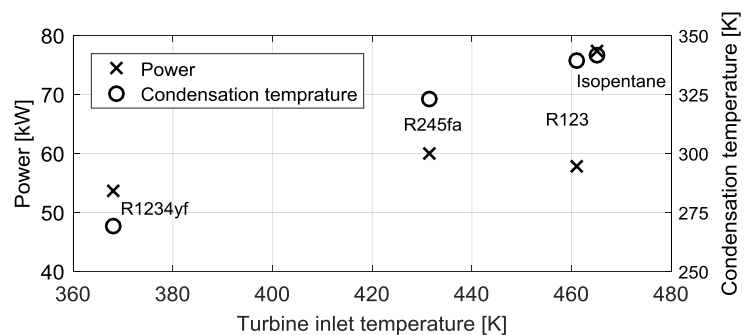
Figure 7. The impact of working fluid replacement on the overall ORC system performance assuming the same flow conditions within the turbine supersonic stator.

7. Conclusions

To realise the widespread implementation of small-scale ORC technology it is necessary to reduce system costs. One way to do this is to develop ORC components that can operate flexibly and with high efficiency with different working fluids, over a wide range operating conditions and in a variety of applications. This paper has investigated the effect of the inlet conditions and of the working fluid on the performance of supersonic converging-diverging nozzles, as simplified models of turbine flow paths. Two supersonic nozzles have been developed using a minimum length method of characteristics design model and the nozzle performance has been verified using CFD. To investigate nozzle performance following a change in the operating conditions, 9 operating cases were defined for each nozzle covering a range of nozzle Reynolds numbers and values for the polytropic index k (P/ρ^k = constant). Predictions for the nozzle performance were made using the similitude model, and also by conserving the amount of flow turning (the Prandtl-Meyer function). Whilst the modified similitude model accurately predicted the nozzle mass flow rate, it is unsuitable for predicting the nozzle outlet

conditions. However, it was found that conserving the Prandtl-Meyer function can lead to reasonably accurate predictions (to within 2%) of the nozzle outlet conditions provided the percentage change in k is less than 10%. Finally, by assuming the nozzle design can be implemented into a suitable turbine design and then ORC system, the possibility of matching the same turbine with different heat sources through working fluid selection has been demonstrated.

References
[1] Colonna, P., Casati, E., Trapp, C., Mathijssen, T., Larjola, J., Turunen-Saaresti., T., and Uusitalo, A., 2015, "Organic Rankine cycle power systems: from the concept to current technology, applications and an outlook for the future", J Eng Gas Turb Power, **137**(10).
[2] Thompson, P., 1971, "Fundamental derivative in gas-dynamics", Physics of Fluids, **14**(90), pp. 1843.
[3] Galiana, F. J. D., Wheeler, A. P. S., and Ong, J., 2015, "A study on the trailing-edge losses in organic Rankine cycle turbines", ASME Turbo Expo 2015, 15-19th June, Montreal Canada.
[4] Moustapha, H., Zelesky, M. F., Baines, N. C., and Japiske, D., 2003, *Axial and Radial Turbines*, Concepts NREC, Inc.
[5] Wheeler, A. P. S. and Ong, J., 2013, "The role of dense gas dynamics on organic Rankine cycle turbine performance", J Eng Gas Turb Power, **135**(10).
[6] Pasquale, D., Ghidoni, A., and Rebay, S., 2013, "Shape Optimization of an Organic Rankine Cycle Radial Turbine Nozzle", J Eng Gas Turb Power, **135**(4).
[7] Hoffren, J., Talonpoika, T., Larjola, J., and Siikonen, T., 2002, "Numerical Simulation of Real-Gas Flow in a Supersonic Turbine Nozzle Ring", J Eng Gas Turb Power, **124**(4).
[8] Harinck, J., Turunen-Saaresti, T., Colonna, P., Rebay, S., and van Buijtenen, J., 2010, "Computational study of a high-expansion ratio radial organic Rankine cycle turbine stator", J Eng Gas Turb Power, **132**(5).
[9] Harinck, J., Pasquale, D., Pecnik, R., Buijtenen, J. V., and Colonna, P., 2013, "Performance improvement of a radial organic Rankine cycle turbine by means of automated computational fluid dynamic design", P I Mech Eng A-J Pow, **227**(6), pp. 637-645.
[10] Wheeler, A. P. S., and Ong, J., 2014, "A study on the three-dimensional unsteady real-gas flows within a transonic ORC turbine", ASME Turbo Expo 2014, 16-20th June, Dusseldorf, Germany.
[11] Spinelli, A., Guardone, A., Cozzi, F., Carmine, M., Cheli, R., Zocca, M., Gaetani, P. and Dossena, V., 2015, "Experimental observation of non-idea nozzle flow of siloxane vapor MDM", 3rd International Seminar on ORC Power Systems, Brussels, Belgium.
[12] Mathijssen, T., Gallo, M., Casati, E., Guardone, A., and Colonna, P., 2015, "Wave speed measurements in non-ideal compressible flows using flexible asymmetric shock tube (FAST)", 3rd International Seminar on ORC Power Systems, Brussels, Belgium.
[13] Cameretti, M. C., Ferrara, F., Gimelli, A., and Tuccillo, R., 2015, "Employing micro-turbine components in integrated solar-MGT-ORC power plants", ASME Turbo Expo 2015, 15-19th June, Montreal, Canada.
[14] Wong, C. S., and Krumdieck, S., 2015, "Scaling of gas turbine from air to refrigerants for organic Rankine cycles using similarity concept", J Eng Gas Turb Power, **138**(6).
[15] Astolfi, M., and Macchi, E., 2015, "Efficiency correlations for axial-flow turbines working with non-conventional fluids", 3rd International Seminar on ORC Power Systems", 12-14th October, Brussels, Belgium.
[16] White, M., and Sayma, A. I., 2015, "The application of similitude theory for the performance prediction of radial turbines within small-scale low-temperature organic Rankine cycles", J Eng Gas Turb Power, **137**(12).
[17] White, M., and Sayma, A.I., 2015, "The impact of component performance on the overall cycle performance of small-scale low temperature organic Rankine cycles", 9th International Conference on Compressors and their Systems, London, UK.
[18] Lemmon, E. W., Huber, M. L., and McLinden, M. O., 2013, *NIST Standard Reference Database 23: Reference Fluid Thermodynamic and Transport Properties-REFPROP,* Version 9.1, National Institute of Standards and Technology, Standard Reference Data Program, Gaithersburg.
[19] Aldo, A. C., and Argrow, B. C., 1995, "Dense gas-flow in minimum length nozzles", Journal of Fluids Engineering, **117**(2), pp. 270-276.